Journal of The Electrochemical Society, **148** (7) F140-F147 (2001)
0013-4651/2001/148(7)/F140/8/$7.00 © The Electrochemical Society, Inc.

X-Ray Photoelectron Spectroscopy of Gate-Quality Silicon Oxynitride Films Produced by Annealing Plasma-Nitrided Si(100) in Nitrous Oxide

H.-W. Chen,[a] D. Landheer,[b,*,z] T.-S. Chao,[c] J. E. Hulse,[b] and T.-Y. Huang[a,c]

[a]*Institute of Electronics Engineering, National Chiao-Tung University, Hsinchu 300, Taiwan*
[b]*National Research Council of Canada, Institute for Microstructural Sciences, Ottawa, Ontario, Canada K1A 0R6*
[c]*National Nano-Device Laboratories, Hsinchu 300, Taiwan*

Ultrathin silicon oxynitride films with thickness in the range of 1.8-3.5 nm have been produced on Si(100) by nitridation of an NO-oxidized surface with an electron-cyclotron resonance plasma source. The films were annealed in N_2O at 950°C for times up to 60 s and formed into Al-gated capacitors for capacitance-voltage (CV) and current-voltage analysis. The rapid annealing increases the oxygen content of the films but results in capacitors with excellent electrical properties. For a plasma oxynitride with equivalent oxide thickness, $t_{eq} = 1.8$ nm, current reductions of ~20 over that for SiO_2 films have been obtained for gate voltages in the range 1-1.5 V. For comparison, the thickness of the oxynitrides was obtained by X-ray photoelectron spectroscopy of the Si 2p, N 1s, and O 1s photoelectrons. By analyzing the yield from thick silicon dioxide and silicon nitride films, the electron escape depth in silicon nitride was estimated to be 1.7 nm for the Si 2p electrons. By correcting the measurements of the oxygen/nitrogen concentration ratio obtained from the O 1s and N 1s XPS peaks, and calculating the dielectric constant with a Bruggeman effective medium approximation, the equivalent oxide thickness was calculated. Agreement to ~0.2 nm was obtained with t_{eq} determined by the CV analysis. Information obtained from the XPS analysis can also give information about bonding configurations and possible errors due to nonuniform stoichiometry as a function of depth.
 [DOI: 10.1149/1.1374219]

Manuscript submitted July 6, 2000; revised manuscript received February 19, 2001. Available electronically May 31, 2001.

Silicon nitride and oxynitrides are being evaluated as replacements for silicon dioxide in the gates of aggressively scaled complementary metal oxide semiconductor (CMOS) devices. Although boron penetration and hot-electron stress effects can potentially be reduced by monolayer quantities of nitrogen, larger nitrogen concentrations result in a higher dielectric constant, allowing for reduction of the direct tunneling currents. Treatment of the Si(100) surface with a nitrogen plasma results in the formation of a defective silicon nitride layer. In order to reduce defects in gate-quality oxynitrides, they are often annealed in nitrous oxide[1] after formation, and this results in an increase in the oxygen content of the films. Previous work has focused on measuring the redistribution of nitrogen at the interface between Si(100) and silicon dioxide films during N_2O annealing,[2] or the effect of long (up to 30 min) oxidations of silicon nitride films in N_2O.[3] The amount of nitrogen left in ultrathin oxynitride films after rapid thermal oxidation in N_2O has not been the subject of much comment by those who measure equivalent oxide thicknesses using capacitance measurements.

A major reason for this is the difficulty of determining the nitrogen profile of ultrathin films since ion-beam techniques such as medium-energy ion scattering,[2] or narrow resonance nuclear reaction analysis[4] are not readily available for routine analysis, while other methods such as secondary ion mass spectrometry[5] have reached their resolution limits. A simple and generally available technique such as X-ray photoelectron spectroscopy (XPS) can give useful information such as the film thickness and the oxygen/nitrogen concentration ratio and can provide a measure of the nonuniformity with depth.

A recent review discusses much of the literature describing the XPS analysis of ultrathin silicon dioxide films.[6] It highlights the sensitivity of ellipsometry measurements to surface contamination in contrast to the XPS technique which involves a ratio of two peak areas equally attenuated by contaminants. XPS measurements on SiO_2 films have also been carefully calibrated against other techniques such as transmission electron microscopy and capacitance-voltage (CV) measurements.[7] Previous work was facilitated by the relative simplicity of growing a number of stoichiometric silicon dioxide films with thicknesses in the range of interest. For silicon nitride films the calibration is more difficult, because it cannot generally be assumed that the nitrogen concentration does not change with film thickness.

In this paper the equivalent oxide thickness of plasma-nitrided films annealed in N_2O at 950°C was determined by CV measurements, and the quality of these films was determined by CV and current-voltage (I-V) measurements. The thickness of N_2O-annealed oxynitride films produced by plasma nitridation and by low-pressure chemical vapor deposition (LPCVD) was determined by analysis of the Si 2p (substrate) and Si 2p (bonded) XPS lines and their composition was determined by analysis of the N 1s and O 1s lines. The electron escape depth of Si 2p electrons from silicon nitride was determined by comparing the yields in thick silicon nitride and silicon dioxide standards. The XPS measurements, coupled with interpolations from the silicon dioxide and silicon nitride standards, were used to self-consistently recalculate the thickness. The dielectric constant determined from a Bruggeman effective medium approximation (EMA)[8] using the oxygen/nitrogen ratio was then used to calculate the equivalent oxide thickness for comparison with the CV measurements. Finally, estimates are made of potential errors in the XPS analysis introduced by assuming that the films have uniform composition with depth.

Experimental

Formation of oxynitrides.—Si(100) wafers (0.025 Ω-cm n-type) were given an HF-last RCA clean prior to film deposition. Two types of silicon oxynitride were studied in this work. One set was formed by first oxidizing the wafers in nitric oxide (NO) at a pressure of 4 mTorr for 6 min at 780°C. Without breaking vacuum, these wafers were exposed to a nitrogen plasma for 5 s at a substrate temperature of 300°C. The plasma was formed using 450 W of absorbed microwave power and 15 sccm of molecular nitrogen in an electron-cyclotron resonance (ECR) apparatus (described previously Ref. 9) positioned 50 cm from the silicon substrates.

Another set of films, produced for comparison purposes, was formed by a standard low-pressure chemical vapor deposition with silane and dichlorosilane at 780°C. These were given a rapid anneal in flowing nitrogen for 30 s at 1000°C to densify the films prior to oxidation.

* Electrochemical Society Active Member.
z E-mail: dolf.landheer@nrc.ca

Oxidation of oxynitrides.—The wafers were introduced into a Heatpulse 610 (Steag RTP Systems) rapid thermal processor (RTP) where they were first heated in flowing nitrogen for 4 min at 500°C to drive off water vapor. The plasma-nitrided wafers were immediately given a 30 s anneal in N_2 at 950°C to densify them prior to the oxidation in N_2O, but this step was omitted for the LPCVD wafers since they were annealed in N_2 immediately after the LPCVD deposition. All the films were oxidized in flowing N_2O at 950°C. To compensate for the optical absorption by N_2O,[10] the RTP pyrometer was calibrated by performing measurements on a test wafer with an embedded thermocouple. The accuracy of the temperature measurement is estimated to be ±25°C.

XPS analysis of oxynitrides.—The analysis of film composition was done using a PHI XPS instrument which employed a nonmonochromatic Mg Kα X-ray source with a hemispherical electron energy analyzer at an angle $\theta = 45°$ from the wafer normal (standard X-ray source position 54.7° from analyzer). Spectra were obtained with a bandpass energy of 23.5 eV, resulting in an energy resolution of ~1 eV.

A technique for background removal, correcting the measured spectra for inelastic scattering, has been formulated by Tougaard[11] in terms of an inelastic scattering cross section which varies with the energy lost as a result of the inelastic scattering. Calculations using the inelastic scattering cross sections for SiO_2 provided in Ref. 11 have been used to evaluate the effect of inelastic scattering. The resultant primary excitation spectra were not significantly different than the spectra obtained from the measured peaks using a linear background correction. This was expected since the inelastic scattering must be small for scattering events that result in energy losses less than the oxynitride bandgap (>5 eV). The analysis of Tougaard[11] has shown that the commonly used Shirley background correction cannot be correct; however, its use would not result in significant changes in the measured intensity ratios, because the background is relatively flat under the main peaks.

The O 1s and N 1s peak areas were obtained from the fits of one or two Gaussian-Lorenzian functions to the observed spectra. The Si 2p peak was fit with two features, *i.e.*, the $2p_{3/2} - 2p_{1/2}$ doublet characteristic of electron emission from the Si substrate and a broader Gaussian-Lorenzian peak due to emission from the overlying film. The doublet was characterized using a Si(100) wafer given an RCA-HF last clean and these features (0.61 eV splitting, 2:1 area ratio, 70% Gaussian-30% Lorentzian lineshape) were used for the fitting of the spectra of the oxynitride films. The fit of the oxynitride Si 2p spectra thus involved optimizing seven parameters, the full width at half maximum intensity (fwhm) of the doublet, its intensity, its position, the intensity of the Si 2p (oxynitride) peak, its fwhm, its position, and the ratio of Gaussian/Lorenzian components in its lineshape.

In the following the subscripts o, n, Si, and on are used to designate parameters for the O 1s, N 1s, Si 2p (substrate), and Si2p (bonded to O and N) features, respectively. It is assumed that the films are homogeneous, and this assumption is investigated in more detail later. Thus λ_o, λ_n, and λ_{on} are the electron escape depths for the O 1s, N 1s, and Si 2p electrons in an oxynitride film, S_o, S_n, and S_{on} are the atomic sensitivity factors, and C_o, C_n, and C_{on} are the concentrations of oxygen, nitrogen, and silicon atoms in the film. The parameter λ_{Si} is the electron escape depth for Si 2p electrons in the silicon substrate, C_{si} is the concentration of silicon atoms in the substrate, and d is the film thickness. The following quantities involving the areas, I_o, I_n, I_{on}, and I_{Si}, of the four features were used in the analysis of the films[12,13]

$$d = \lambda_{on} \cos(\theta) \ln[I_{on}/\beta_{on}I_{Si} + 1] \quad [1]$$

$$R = \frac{C_o}{C_n} = \frac{I_o S_n[1 - \exp(-d/\lambda_n \cos\theta)]}{I_n S_o[1 - \exp(-d/\lambda_o \cos\theta)]} \quad [2]$$

$$\frac{C_o}{C_{on}} = \frac{I_o S_{on}[1 - \exp(-d/\lambda_{on} \cos\theta)]}{I_{on} S_o[1 - \exp(-d/\lambda_o \cos\theta)]} \quad [3]$$

and

$$\frac{C_n}{C_{on}} = \frac{I_n S_{on}[1 - \exp(-d/\lambda_{on} \cos\theta)]}{I_{on} S_n[1 - \exp(-d/\lambda_n \cos\theta)]} \quad [4]$$

where $\beta_{on} = \lambda_{on}C_{on}/\lambda_{Si}C_{si}$. The sensitivity factor ratios in Eq. 1-3 are related to the escape depths[12] by $S_o/S_{on} = T_o\lambda_o/T_{on}\lambda_{on}$ and $S_n/S_{on} = T_n\lambda_n/T_{on}\lambda_{on}$, where T_o, T_n, and T_{on} are the transmission of the electron analyzer at the energies of the O 1s, N 1s, and Si 2p electrons, respectively. The escape depths were calculated for the O 1s and N 1s electrons from those for the Si 2p electrons using the following expressions

$$\lambda_o = \lambda_{on}(720/1150)^m \text{ and } \lambda_o = \lambda_{on}(855/1150)^m \quad [5]$$

where the O 1s, N 1s, and Si 2p electrons have energies of 720, 855, and 1150 eV, respectively. A value of $m = 0.5$ has been used by Seah and Dench[14] and a value of $m = 0.7$ gives a good fit to the data of Tanuma *et al.*[15] In fact, choosing any value between $m = 0.5$ and $m = 0.7$ results in negligible changes in the calculated values of d, and changes in R of <1.5%. With the use of Eq. 5, the sensitivity factor ratios become independent of oxynitride film composition, as is often assumed.

To calibrate the XPS thickness measurements, spectra were obtained from thick SiO_2 and silicon nitride films. The former was a thermal oxide grown at 1050°C in O_2, while the latter was a high-quality silicon nitride film deposited using a plasma-CVD process[9] which results in a [N]/[Si] ratio of 1.37, as determined by nuclear reaction analysis (NRA) and Rutherford backscattering (RBS) measurements of the nitrogen and silicon contents, respectively. This sample is slightly nitrogen-rich, consistent with the <5% atom % hydrogen bonded as NH.[9] The density of silicon dioxide was taken as 2.27 g/cm^3 [16] corresponding to a density of silicon atoms $C_{ox} = 2.28 \times 10^{22}$ atom/cm^3. The density of the silicon nitride film was determined from the NRA and RBS measurements and the thickness obtained by ellipsometry.[9,17] This gave a value for the density of 2.95 g/cm^3 which corresponds to a silicon concentration $C_{nit} = 3.80 \times 10^{22}$ atom/cm^3. The nitride wafer was given a 30 s clean in 1% HF solution, rinsed, and blown dry, and the substrates were placed side-by-side on a metal mount along with a piece of Si(100) given an RCA HF-last clean. Spectra were obtained for all three samples, taking care to ensure that the spectrometer alignment and incident X-ray intensity was the same for all three.

Since the films of interest had excellent electrical properties after annealing, it was assumed that the oxynitrides, consisting of molecules of SiO_xN_y, were free of O-N, Si-Si, and dangling bonds, *i.e.*, that $x/2 + 3y/4 = 1$ (Mott's law, Ref. 18). It follows that x is related to the oxygen/nitrogen concentration ratio, R, by $x = 4R/(3 + 2R)$. In Appendix A it is shown that the escape depth in an oxynitride film can be given to a good approximation by a linear interpolation between those for pure silicon dioxide and nitride films, λ_{ox} and λ_{nit}, respectively, viz.

$$\lambda_{on} = \frac{x\lambda_{ox} + (2 - x)\lambda_{nit}}{2} = \frac{2R\lambda_{ox} + 3\lambda_{nit}}{(3 + 2R)} \quad [6]$$

Finally, it is shown that β_{on} differs by <5% for silicon nitride and silicon dioxide so only a small error is introduced by using the following linear interpolation between the values for pure silicon dioxide and nitride films, β_{ox} and β_{nit}, respectively

$$\beta_{on} = \frac{x\beta_{ox} + (2 - x)\beta_{nit}}{2} \quad [7]$$

Since the electron escape depths depend on the oxygen/nitrogen ratio, and the determination of the latter depends on the calculated thickness, we have used a simple iterative procedure to calculate x and d. It uses pure silicon dioxide values as the initial guesses for λ_{on} and β_{on}. The iterations, which can be carried out on a simple spreadsheet, involve calculating Eq. 1, 2, 5, 6, and 7 and then repeating the sequence starting at Eq. 1. Convergence to $<0.1\%$ can be obtained after two or three iterations.

Electrical measurements.—Al-gated capacitors were made by evaporating aluminum through a shadow mask followed by annealing in forming gas at 380°C for 20 min and back contacts were made with In-Ga eutectic. The area of the capacitors, $\sim 5 \times 10^{-4}$ cm^2, was measured to an accuracy of $\pm 2\%$ with a calibrated digitizing camera. Electrical measurements were made by probing the Al gates in a probe station attached to two instruments, a multifrequency LCR meter (HP model 4275A), and a picoammeter/dc voltage source (HP model 4140B). High frequency CV measurements were made by stepping with 0.1 V steps each second, first from -3 to $+3$ V and then in the reverse direction to look for hysteresis. IV characteristics were obtained with the picoammeter by stepping the voltage source from 0 V in a positive direction (toward accumulation) until breakdown, which was characterized by a steep rise to currents above 10^{-2} A. The equivalent oxide thickness was obtained from the 100 kHz CV characteristics by using the NCSU CV fitting routine[19] which includes quantum effects in the channel.

Hajii *et al.*[8] have used a Bruggeman effective medium approximation to estimate the dielectric constant, κ_{oxnit}, of oxynitride films in terms of the value of x

$$\kappa_{oxnit} = 8.85 - 4.82x + 0.89x^2 \qquad [8]$$

The coefficients were determined for oxynitride films produced by LPCVD with low oxygen contents, but the estimate has been used here for our films with higher values of x. The equivalent oxide thickness, d_{eq}, was calculated from the XPS thickness using the relationship $d_{eq} = 3.85d/\kappa_{oxnit}$.

Results

Characteristics of the N 1s XPS peak.—The N 1s spectra for some of the plasma-nitrided samples are shown in Fig. 1a and the fit of a single peak to a spectrum is shown in Fig. 2a for the sample given a 15 s anneal in N_2O. The deviation between the measured spectrum (solid circles) and the fit peak (solid line) is shown by the dotted line (residual errors). With one exception, all the N 1s spectra were well fit by one peak. The N_2 plasma increases the fwhm of the N 1s spectrum from 1.46 to 1.73 eV, and for this spectrum a better fit is produced using two peaks, one at 398.3 eV with 31% of the total area, and the other at 398.8 eV. Subsequent annealing reduces the fwhm to 1.57 eV, as shown in Table I. The peaks were referenced to the Si $2p_{3/2}$ substrate peak at 99.9 eV, so sample charging or bandbending in the Si substrate could contribute to the small shifts from 398.3 to 398.8 eV shown in Table I. The high-resolution XPS measurements of Hussey *et al.*[20] identified two components in this energy range, a 398 eV peak assigned to Si_3N_4, and a 398.8 eV assigned to an oxynitride species of the form N-Si-O. Others have ascribed a peak at 398.6 eV to bonding states where each N atom is bonded to only two Si atoms, leaving a nitrogen dangling bond.[21] No feature near 400.7 eV attributable to N-O bonds[22] was observed in any of the plasma-nitrided films after annealing in N_2O.

The N 1s peak was at 398.5 eV for all the LPCVD samples, the fwhm was 1.70 eV before N_2O oxidation, and the fwhm was 1.66 $\pm$ 0.01 eV for all the oxidized LPCVD samples. The main peak was fitted with one component, and there was no peak near 400.7 eV attributable to N-O bonds. However, the LPCVD films showed a small satellite, which was observable after the N_2O oxidation, with $<0.3\%$ of the area of the main peak situated at 4.2 eV to the high binding energy side of the main peak. This feature has previously been attributed to screening effects associated with the formation of islands of SiO_2 at the interface.[23]

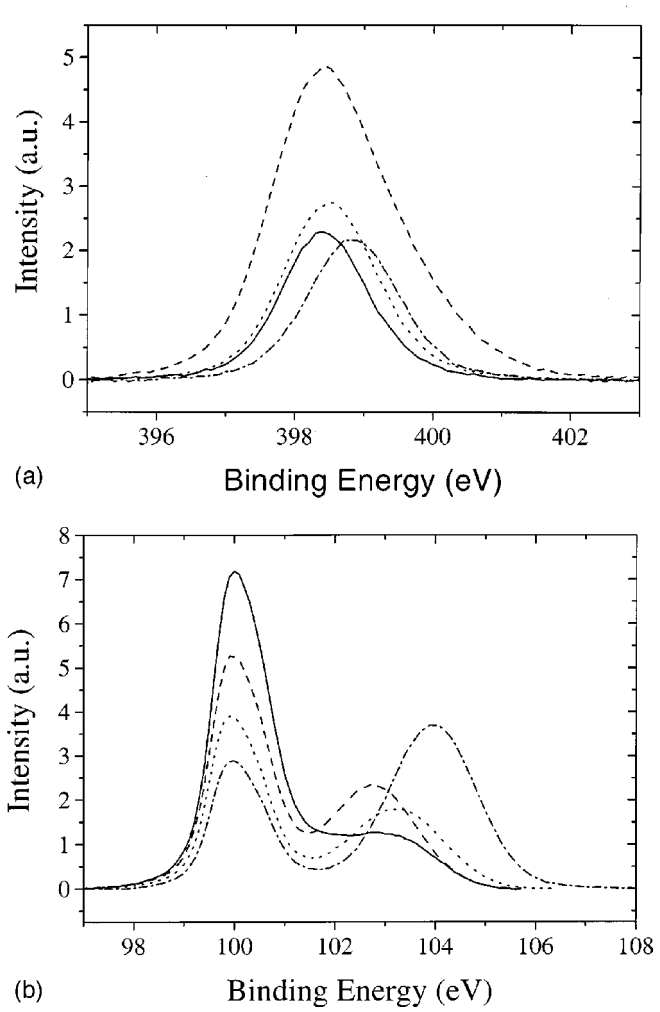

Figure 1. (a, Top) N 1s spectra and (b, bottom) Si 2p spectra of plasma nitrided films at various stages of processing: (——) after oxidation of Si(100) in NO at 780°C, (— — —) after exposure to N_2 plasma, (· · · ·) after 30 s anneal in N_2 at 950°C, (— · — · — · —) after 60 s anneal in N_2O at 950°C.

The Si 2p spectra for the plasma-nitrided films are shown at various stages of processing in Fig. 1b. The spectral decomposition of the spectrum for the plasma-nitrided film after a 15 s oxidation in N_2O is shown in Fig. 2b with the background removed. The sum of the residual errors for the fits are typically $<0.3\%$ of the area of the measured peak areas for all the films after annealing in N_2 or N_2O at 950°C. The residuals could be reduced by the addition of more components to the fits, but the improvements were not statistically significant. The maximum errors in the area ratio of the Si 2p (bonded) to the Si 2p (substrate) peaks were estimated to be $\sim \pm 10\%$.

XPS calibration.—Analysis of the O 1s signal from the silicon nitride sample indicated that there was approximately an amount of oxide on the nitride surface that would be contained in a 0.12 nm layer of silicon dioxide. Since a heater or sputter gun were not available on the XPS system to remove this contamination, which was probably water and oxide,[24] the measured peak areas were corrected by assuming there was a 0.12 nm thick fictitious layer on the surface of both the oxide and nitride standards that absorbed like silicon dioxide but contained no silicon. The sensitivity ratio ob-

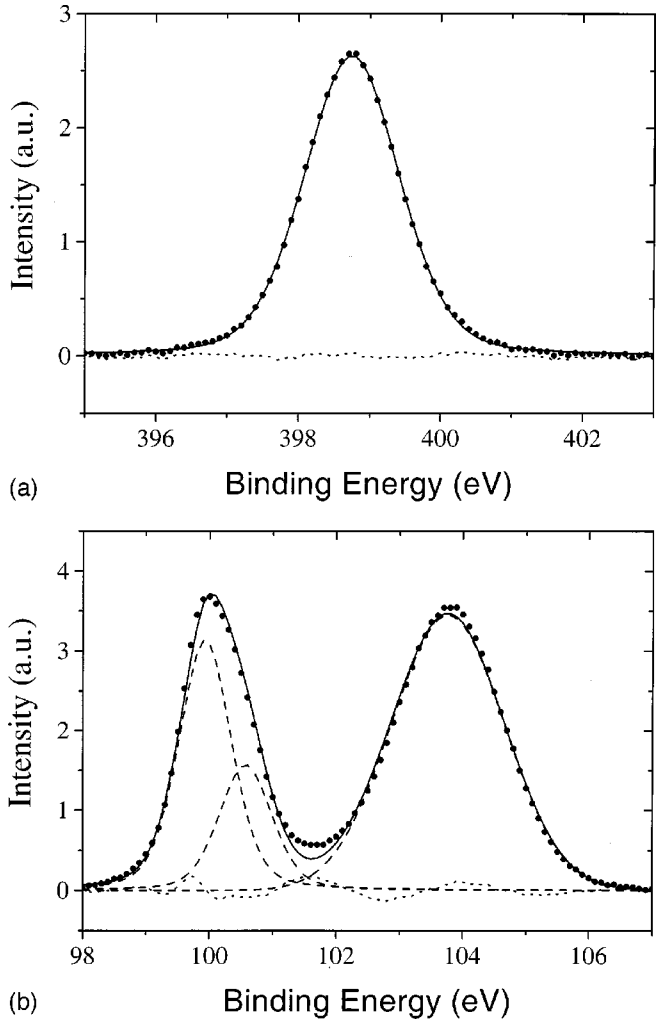

Figure 2. (a, top) N 1s spectrum and (b, bottom) Si 2p spectrum with background removed for plasma-nitrided film after 15 s anneal in N_2O at 950°C: (●●●) measured, (— — —) fit peaks, (——) sum of fit peaks, (· · · ·) residual errors.

tained from the nitride standard was $S_n/S_{on} = 1.59$, and that from the silicon dioxide standard was $S_o/S_{on} = 2.54$, resulting in $S_o/S_n = 1.59$.

The Si 2p spectra for the oxide and nitride standards, shown in Fig. 3, are remarkably similar. The intensities, I_{ox} and I_{nit} of the main Si 2p peak near 103 eV were obtained by integration using a linear background which, as discussed above, is consistent with Tougaard's background correction technique.[11] This gave $I_{nit}/I_{ox} = 0.97 \pm 0.04$. For SiO_2, the value of $\beta_{ox} = 0.75$ and $\lambda_{ox} = 2.96$ nm were taken from Ref. 7, and the values, $\beta_{nit} = 0.73$ and $\lambda_{nit} = 1.73$ nm, were calculated using the relationship $\beta_{nit}/\beta_{ox} = I_{nit}/I_{ox} = (\lambda_{nit}C_{nit})/(\lambda_{ox}C_{ox})$. The calculated Si 2p electron escape depth for silicon nitride is 33% smaller than the value of 2.59 nm obtained from the parameters of Seah and Dench.[14]

Table I. FWHM and binding energy (BE) of the N 1s XPS peak for plasma-deposited silicon oxynitride films after various process steps during formation and after annealing at 950°C in N_2O.

Process	fwhm (eV)	BE (eV)
NO at 780°C for 6 min	1.46	398.3
N_2 plasma at 300°C for 5 s	2.11	398.6
Anneal at 950°C in N_2 for 30 s	1.60	398.6
15 s in N_2O	1.58	398.7
20 s in N_2O	1.57	398.8
30 s in N_2O	1.57	398.8
60 s in N_2O	1.57	398.8

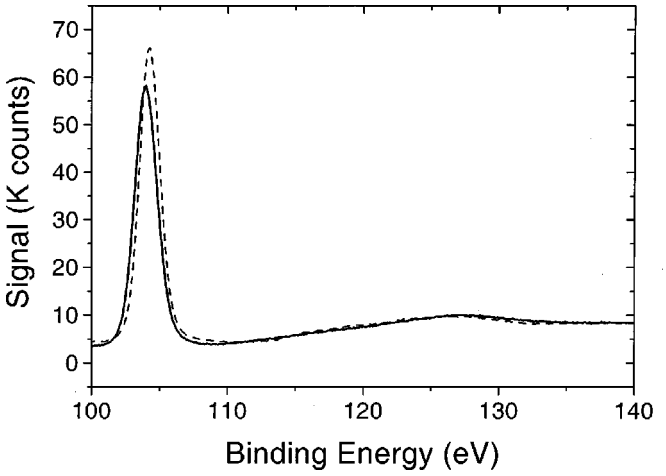

Figure 3. XPS spectra of thick silicon dioxide (— — —) and silicon nitride films (——) showing the Si 2p features and associated peaks caused by inelastic scattering.

For comparison with prior studies, the broad feature between 109 and 140 eV in Fig. 3 associated with inelastic scattering was integrated using a Shirley background. The yields, Y_{ox} and Y_{nit}, were estimated for the oxide and nitride films, respectively, by taking the ratios of the main peak intensity to the sum of the intensities of the main and plasmon peaks, $I_{nit}(\infty)$ or $I_{ox}(\infty)$, for the nitride and oxide samples. The results were $I_{nit}(\infty)/I_{ox}(\infty) = 1.03 \pm 0.04$, $Y_{ox} = 0.70$ and $Y_{nit} = 0.68$. The value for SiO_2 is identical to that found in Ref. 7. The yields were not used in our analysis.

Thickness and composition of annealed films.—Figures 4 and 5 show the calculated thickness (solid circles) and oxygen/nitrogen

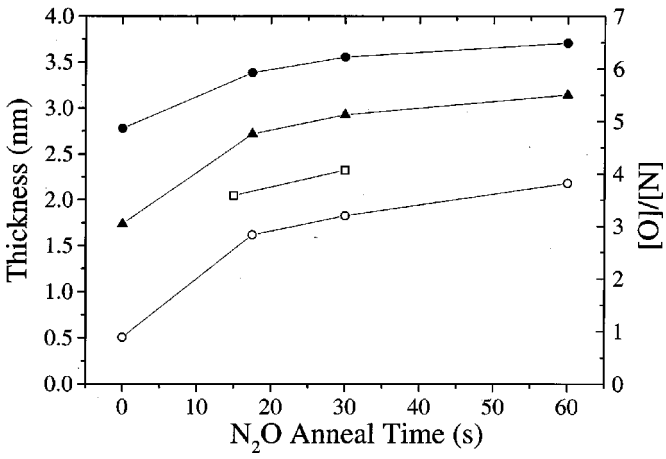

Figure 4. Thickness and oxygen/nitrogen concentrations ratio as a function of annealing time in N_2O at 950°C for silicon oxynitride films deposited by LPCVD on Si(100): (●) thickness from XPS, (▲) equivalent oxide thickness determined from XPS measurements and calculated dielectric constant, (○) [O]/[N] from XPS measurements, (□) XPS thickness for Si(100) oxidized in N_2O at 950°C.

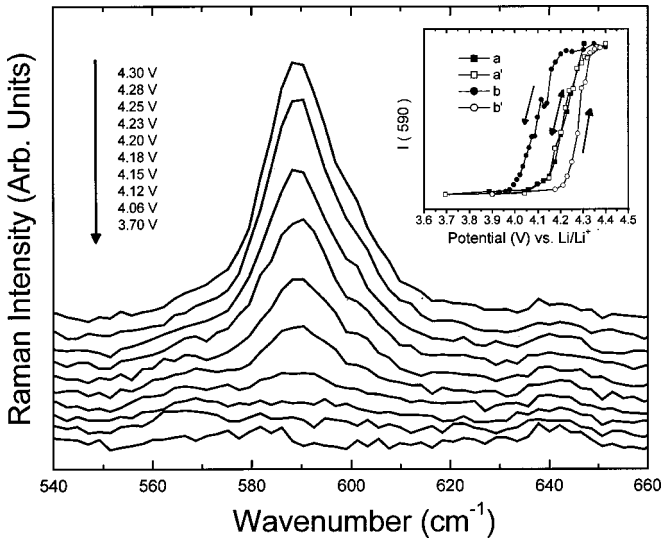

Figure 5. Thickness and oxygen/nitrogen concentrations ratio as a function of annealing time in N_2O at 950°C for silicon oxynitride films formed by oxidation of Si(100) in NO followed by plasma nitridation: (●) thickness from XPS, (♦) thickness from XPS uncorrected for nitrogen, (■) equivalent oxide thickness determined by electrical measurements, (▲) equivalent oxide thickness determined from XPS measurements, (○) [O]/[N] from XPS measurements.

concentration ratios (open circles) as a function of N_2O annealing time for the LPCVD and plasma-nitrided films, respectively. Before oxidation in N_2O the silicon oxynitride film formed by plasma nitridation had an oxygen/nitrogen concentration ratio, $R = 1.9$. The film deposited by LPCVD initially had more nitrogen but was not pure nitride (with $R = 0.9$), likely due to water vapor in the LPCVD furnace or the RTP system used for the postdeposition anneal at 1000°C. The LPCVD oxynitride films increased in thickness during the first 20 s by only 0.9 nm and the plasma-nitrided films increased by 1.0 nm during the same time. The more rapid oxidation of the plasma-nitrided films even though they initially have more oxygen is probably due to the fact that they are thinner.

In Fig. 4 the thickness of a film formed by directly oxidizing a Si(100) wafer given a RCA-HF last clean is shown, for comparison, by the open squares. The oxidations were done for 15 and 30 s at 950°C in N_2O. The thicknesses are in agreement with the N_2O oxidation measurements of Ting *et al.*,[25] confirming the calibration of our pyrometer. XPS measurements indicate a low nitrogen concentration, as expected, with an N 1s peak position at 398.7 eV and a fwhm of 1.65 eV. Comparing these results with the results for the plasma-nitrided films in Fig. 5 and Table I indicates that, for comparable oxidation times at 950°C, the plasma-nitrided and oxidized films have lower equivalent thicknesses than the films produced by oxidizing bare Si(100) substrates in N_2O, have a much higher nitrogen concentration, and a smaller fwhm indicative of more ordered bonding arrangements.

The equivalent oxide thickness, shown by the solid triangles in Fig. 4 and 5, was calculated from the dielectric constant and XPS thickness. For the plasma-nitrided films in Fig. 5, these can be compared to the equivalent oxide thickness obtained from the CV measurements (solid squares). There is agreement to within 0.2 nm. For the LPCVD films, a higher leakage current interfered with the CV measurements and a reliable equivalent thickness could not be obtained in this manner. The leakage in the LPCVD films might be associated with the presence of silicon dioxide islands at the silicon interface deduced from the N 1s spectra. It is also worth pointing out that Song *et al.*[1] annealed their LPCVD films in ammonia prior to N_2O oxidation to reduce their leakage currents.

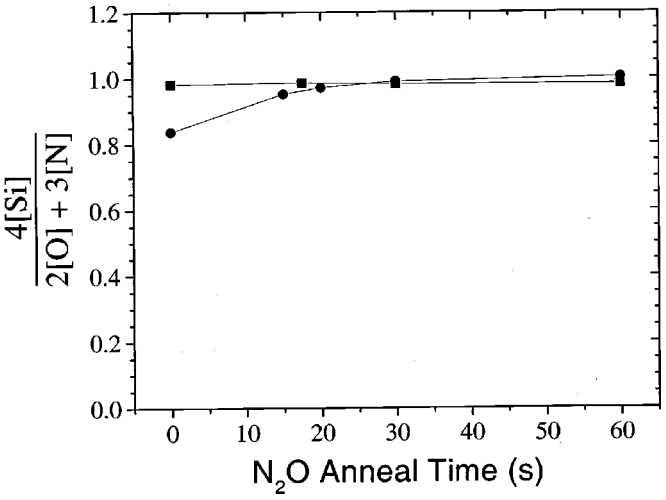

Figure 6. Magnitude of $4[Si]/(2[O] + 3[N])$ calculated using the XPS measurements for the plasma-nitrided (●) and LPCVD (■) films as a function of annealing time in N_2O at 950°C. For films with no N-O bonds and all Si fully bonded to O and N, $4[Si]/(2[O] + 3[N]) = 1$.

In Fig. 5 the thickness obtained from the XPS measurements using Eq. 1 with the values of λ_{ox} and β_{ox} for pure silicon dioxide films is shown for comparison (solid diamonds). The differences between these raw thickness values and those calculated using the values corrected for composition are <0.3 nm over the whole range of oxidation times. The corrections will be more significant for films with lower values of R.

The quantity $4/(2x + 3y) = 4[Si]/(2[O] + 3[N]) = 4C_{on}/(C_o + 3C_n)$ can be calculated using Eq. 3 and 4 and a value of 1 is expected for ideal oxynitride films obeying Mott's law[18] (no Si-Si, O-N, or dangling bonds). Except for the plasma-nitrided film before N_2O oxidation, the values shown in Fig. 6 are close to 1, confirming the calibration of our XPS measurements and the high quality of the films.

Figures 7 and 8 show the 100 kHz capacitance per unit area and current density, respectively, as a function of applied voltage for a plasma-nitrided film with an equivalent oxide thickness of 1.8 nm formed by annealing in N_2O at 950°C for 20 s. No hysteresis was observed between the forward and reverse CV sweeps. Figure 7 also

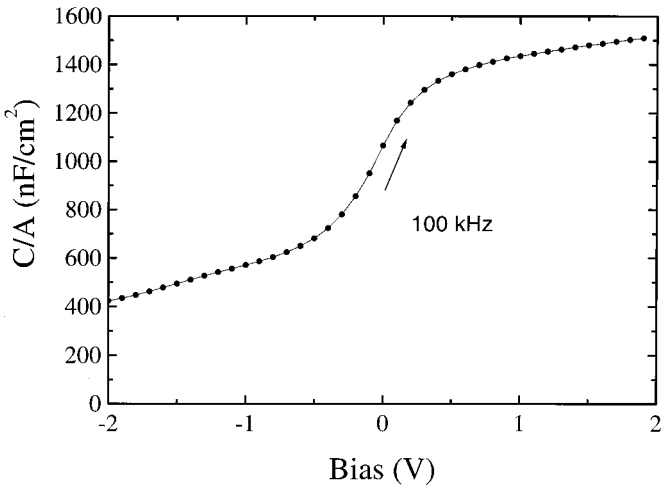

Figure 7. Capacitance per unit area at 100 kHz *vs.* voltage for plasma nitride film annealed for 30 s in N_2O at 950°C: (●) measured, (——) fit from NCSU CV program.[19]

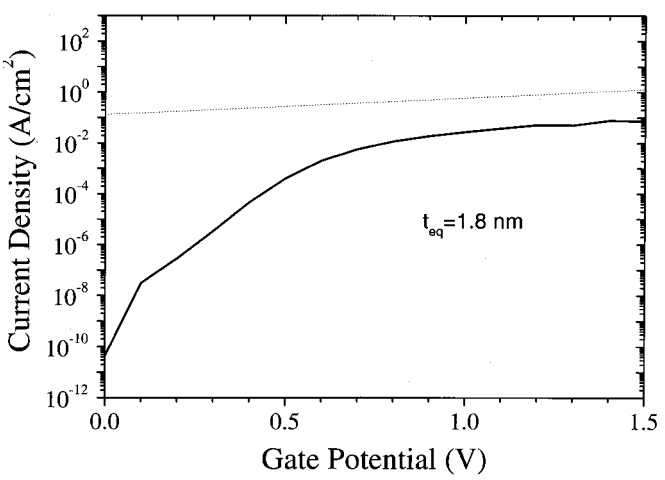

Figure 8. Current density *vs.* voltage for plasma nitride film annealed for 30 s in N_2O at 950°C: (——) measured, (· · · ·) calculated from expression of Brar *et al.*[26]

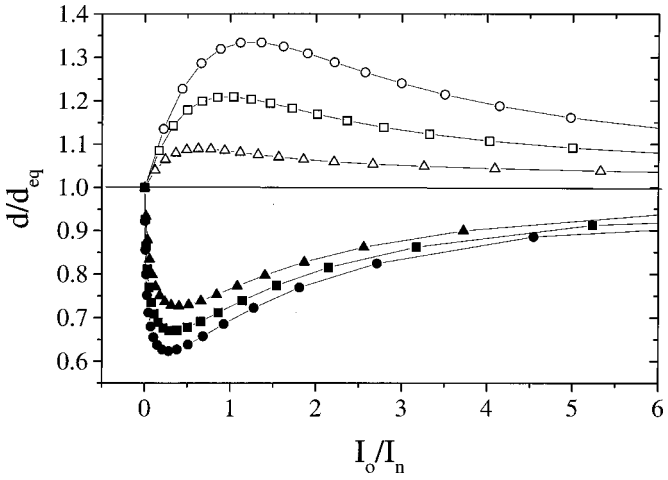

Figure 9. Calculated XPS thickness, d, divided by equivalent oxide thickness, d_{eq}, for films consisting of a layer of silicon dioxide on top of a layer of silicon nitride (open symbols) or a layer of silicon nitride on silicon dioxide (solid symbols): (●) d_{eq} = 2.0 nm, (■) d_{eq} = 1.5 nm, (▲) d_{eq} = 1.0 nm.

shows the result of the fit from the NCSU CV program used to obtain t_{eq} and Fig. 8 shows the current density for a silicon dioxide film with the same equivalent thickness obtained from the expression of Brar *et al.*[26] The oxynitride film has lower currents by a factor of 18 at 1 V and 22 at 1.5 V than a SiO_2 film with the same d_{eq} and breakdown occurred at 3.5 V. The current reductions are lower than the factor of 100 reduction achieved by Song *et al.*[1] for a N_2O annealed LPCVD nitride with comparable t_{eq}, and this may reflect a lower nitrogen concentration in our films since they were not annealed in ammonia prior to oxidation.

Discussion

The analysis presented here assumes a uniform stoichiometry throughout the films. To estimate the errors that could be introduced by this assumption, simulations of the O 1s, N 1s, and Si 2p intensities were done for films having equivalent thickness, d_{eq}, assuming that all the nitrogen is bonded as an Si_3N_4 layer with a thickness, d_n, under a layer of SiO_2 with a thickness d_o. The equations used are given in Appendix B, and similar equations apply for the other extreme where all the SiO_2 is in a layer situated under a Si_3N_4 layer. The ratio $f = d_o/(d_o + d_n)$ must satisfy the requirement that $d_{eq} = 3.85d_n/8.85 + d_o = d_o(1 + 0.435/f - 0.435)$, where the dielectric constants for silicon nitride and silicon dioxide, 3.85 and 8.85, respectively, were obtained from Eq. 8. For each pair, f and d_{eq}, the ratios I_o/I_n and $(I_{sin} + I_{sio})/I_{si}$ were calculated, where I_{sio} and I_{sin} are the intensities of the Si 2p (bonded) peak from the pure SiO_2 and Si_3N_4 layers, respectively. These ratios were treated as experimental inputs to the iterative solution of Eq. 1, 2, 5, 6, and 7 to get a self-consistent value of d and R, *i.e.*, the values of d and R our method would deduce from the simulated peak intensities. Figure 9 shows plots of d/d_{eq} *vs.* R for d_{eq} = 1.0, 1.5, and 2.0 nm. The solid symbols pertain to the case where the nitride sits on top, and for the open symbols the oxide sits on top. The results show that the extreme distributions can result in large errors, but the errors become less significant for films with smaller d_{eq}. For the plasma-nitrided films used for the CV analysis, $d_{eq} \simeq 1.8$ nm and $R > 3$, so that errors of up to 25% in the calculated equivalent oxide thickness are possible. The close agreement between the values calculated from the XPS and CV measurements indicates that our plasma-nitrided films have a relatively uniform nitrogen distribution, or that the centroid of nitrogen concentration is near the center of the film.

Obtaining nitrogen depth profiles for such thin films by angle-dependent XPS measurements or by the medium-energy ion-scattering technique available at a few research institutions could be used to verify this conclusion, but these techniques were not readily available and beyond the scope of this work.

Conclusions

Thin oxynitride films on Si(100) substrates have been oxidized in N_2O at 950°C for times up to 60 s to emulate a process commonly used to improve the quality of gate insulators being developed for deep submicrometer CMOS technology. A considerable oxidation is observed to take place on this time scale with oxygen/nitrogen ratios increasing from one through four for the LPCVD films and from two through six for the plasma-nitrided films. The concomitant increase in equivalent oxide thickness has been determined by CV analysis, where leakage currents were low enough to perform reliable measurements at 100 kHz. The equivalent oxide thickness determined by correcting the XPS thickness for the dielectric constant (calculated from the oxygen/nitrogen ratio and an EMA) were 0.2 nm larger. A 10% error in the intensity ratios can account for 60% of this discrepancy. Another possible source of the difference may be the assumed silicon nitride density which was obtained from the silicon nitride standard. This density may not be appropriate for the calculations of the escape depths in silicon oxynitrides. However, an error in the silicon nitride density would produce a discrepancy which decreases with the [O]/[N] ratio, contrary to what is observed in Fig. 5. A larger difference would result from a nonuniform distribution of nitrogen through the films.

By analyzing the photoelectron yield from thick silicon dioxide and silicon nitride films, the electron escape depth in silicon nitride was estimated to be 1.7 nm. Some of the approximations developed to determine the thickness of the films by XPS could be refined. It would be worthwhile to determine the electron escape depths in silicon nitride or oxynitrides directly by comparing thickness measurements of uniform ultrathin films with TEM measurements. This would require a technique for reliably producing stoichiometric silicon nitride films or uniform oxynitride films with varying thickness. However, the approximations used to extrapolate the electron escape depth for oxynitride from that previously determined for silicon dioxide are not expected to lead to significant errors in this work since the oxidized films had relatively large oxygen/nitrogen ratios. Of more concern is the use of the Bruggeman effective medium approximation which has only been verified for higher nitrogen concentrations than that obtained for this work.[8]

Finally, we have shown that plasma nitridation of NO-oxidized Si(100) using an ECR nitrogen plasma is capable of producing high-

quality gate dielectrics. For a plasma oxynitride with $t_{eq} = 1.8$ nm we have achieved current reductions of ~20 for gate voltages in the range 1-1.5 V. Further analysis of these plasma-nitrided films on MOSFETs with polysilicon gates would be worthwhile.

Acknowledgments

We are indebted to the staff of the National Nano Device Labs and E. Estwick for assistance in the preparation of the samples. We also wish to thank J. R. Hauser for use of the NCSU CV analysis program and W. N. Lennard for the RBS and NRA measurements on the silicon nitride standards. This work was supported by the National Science Council of the Republic of China under contract no. NSC89-2215-E-009-071.

The National Research Council of Canada assisted in meeting the publication costs of this article.

Appendix A

A Linear Approximation for λ_{on}

In this Appendix a linear interpolation for the electron escape depth in silicon oxynitride, λ_{on}, is derived in terms of the electron escape depths in pure silicon dioxide and nitride, λ_{ox} and λ_{nit}, respectively. An interpolation of the oxynitride molecular volume from the molecular volumes V_{ox} and V_{nit}, respectively, of the constituents SiO_2 and $SiN_{4/3}$ can be used for an oxynitride obeying Mott's law, viz.

$$V_{oxnit} = \frac{x}{2} \cdot V_{ox} + \frac{(2-x)}{2} \cdot V_{nit} = \frac{3}{3+2R} \cdot V_{nit} + \frac{2R}{3+2R} \cdot V_{ox} \qquad [A\text{-}1]$$

Since the energy of the Si 2p photoelectrons is relatively large ($E = 1150$ eV), the simple relationship tabulated by Seah and Dench[14] can be used to relate the scattering mean-free path (in nanometers) for the oxynitride, $\lambda_{on} = 0.72a^{3/2}E^{1/2}$, where the monolayer thickness (in nanometers), $a = [V_{oxnit}/(1+x+y)]^{1/3}$, and V_{oxnit} is the volume of the oxynitride molecule with composition SiO_xN_y. This results in an estimate for the mean-free path for the oxynitride

$$\lambda_{on} = 0.72E^{1/2}\left[\frac{3V_{nit} + 2R \cdot V_{ox}}{(7+6R)}\right]^{1/2} = 0.72E^{1/2}\left[\frac{3(1-x/2) \cdot V_{nit} + 3x/2 \cdot V_{ox}}{(7+x)}\right]^{1/2} \qquad [A\text{-}2]$$

The molecular volumes V_{ox} and V_{nit} were estimated from the densities of SiO_2 and Si_3N_4, 2.27 and 2.95 g/cm^3, respectively. The values of mean-free path calculated using this relation are $\lambda_{nit} = 2.59$ nm and $\lambda_{ox} = 2.93$ nm, for silicon nitride and silicon dioxide, respectively. The calculations show that between these limits a simple linear interpolation, $\lambda_{on} = x/2 \cdot \lambda_{ox} + (1-x/2) \cdot \lambda_{nit}$, results in deviations from Eq. A-2 of no larger than 1%. This justifies the use of a linear interpolation for the oxynitride films; however, since the measured electron escape depths for silicon dioxide and silicon nitride films differ from those calculated above, the experimental values of λ_{ox} and λ_{nit} have been used in the interpolation for λ_{on}.

Appendix B

Intensities for Two-Layer Films

In this Appendix the intensities of the O 1s, N 1s, Si 2p peaks are calculated assuming a film having an equivalent oxide thickness, d_{eq}, is composed of two layers, one pure oxide with thickness d_o and a dielectric constant of 3.85, and the other pure nitride with thickness d_n and dielectric constant of 8.85. The thicknesses of the two layers are fixed by d_{eq} and a specification of the fraction of the total thickness, f, which is silicon dioxide

$$d_o = \frac{8.85 f d_{eq}}{8.85f + 3.85(1-f)} \text{ and } d_n = \frac{8.85(1-f)d_{eq}}{8.85f + 3.85(1-f)} \qquad [B\text{-}1]$$

Assuming the silicon nitride layer sits underneath the silicon dioxide layer, the following standard equations can be written[12,13]

$$I_o = S_o C_o [1 - \exp(-d_o/\lambda_o \cos\theta)] \qquad [B\text{-}2]$$

$$I_n = S_n C_n [1 - \exp(-d_n/\lambda_n \cos\theta)] \exp(-d_o/\lambda_{n,ox} \cos\theta) \qquad [B\text{-}3]$$

$$I_{Si} = S_{Si} C_{Si} \exp(-d_n/\lambda_{nit} \cos\theta) \exp(-d_o/\lambda_{ox} \cos\theta) \qquad [B\text{-}4]$$

$$I_{sio} = S_{ox} C_{ox} [1 - \exp(-d_o/\lambda_{ox} \cos\theta)] \qquad [B\text{-}5]$$

and

$$I_{sin} = S_{nit} C_{nit} [1 - \exp(-d_n/\lambda_{nit} \cos\theta)] \exp(-d_o/\lambda_{ox} \cos\theta) \qquad [B\text{-}6]$$

where $\lambda_{n,ox}$ is the escape depth for the N 1s electrons in silicon dioxide. Assuming, again, that the escape depths scale with $E^{1/2}$,[14] gives $\lambda_{n,ox} = \lambda_{ox}(855/1150)^{1/2}$. Similar equations can be derived for the case where the silicon nitride is on top of the silicon dioxide.

List of Symbols

$a = [V_{oxnit}/(1+x+y)]^{1/3}$	the monolayer thickness (in nanometers) of the molecule SiO_xN_y
C_o, C_n, C_{on}	concentration of oxygen, nitrogen, and silicon atoms in silicon oxynitride
C_{ox}, C_{nit}	the concentration of Si in silicon dioxide and nitride standards
C_{Si}	concentration of silicon atoms in silicon substrate
$d_{eq} = 3.85d/\kappa_{oxnit}$	equivalent oxide thickness from XPS measurements
d_o, d_n, d	thickness of silicon dioxide, nitride, and oxynitride films for XPS measurements
E	photoelectron energy
I_o, I_n	area of the O 1s and N 1s XPS peaks
$I_{ox}(\infty)$, $I_{nit}(\infty)$	intensity of the Si 2p peak, including plasmon contributions, for silicon dioxide and nitride standards.
I_{sio}, I_{sin}, I_{on}	area of the Si 2p (bonded) XPS peak in silicon dioxide, nitride, or oxynitride
I_{Si}	area of the Si 2p XPS doublet from the Si(100) substrate
$R = C_o/C_n$	oxygen/nitrogen concentration ratio
S_o, S_n, S_{on}	atomic sensitivity factors used to calculate oxygen, nitrogen, and silicon concentrations from the O 1S, N 1s, and Si 2p (bonded) XPS peak areas
S_{Si}	atomic sensitivity factor used to calculate the silicon concentration in the silicon substrate
t_{eq}	equivalent oxide thickness from CV measurements
T_o, T_n, T_{on}	transmission of the electron analyzer at the energies of the O 1s, N 1s, and Si 2p electrons
V_{ox}, V_{nit}, V_{oxnit}	the molecular volumes of silicon oxide, nitride, and oxynitride.
x, y	number of oxygen and nitrogen atoms, respectively, in a molecule of SiO_xN_y

Greek

κ_{oxnit}	dielectric constant of oxynitride
λ_{ox}, λ_{nit}, λ_{on}	Si 2p electron escape depth from silicon dioxide, nitride, and oxynitride
λ_o, λ_n	O 1s and N 1s XPS electron escape depths from silicon oxynitride

References

1. S. C. Song, H. F. Luan, Y. Y. Chen, M. Gardner, J. Fulford, M. Allen, and D. L. Kwong, *Tech. Dig. Int. Electron Devices Meet.*, **98**, 373 (1998).
2. E. P. Gusev, H. C. Lu, E. Garfunkel, T. Gustafsson, and M. L. Green, *IBM J. Res. Dev.*, **43**, 265 (1999), and references cited therein.
3. N. S. Saks, D. I. Ma, and W. B. Fowler, *Appl. Phys. Lett.*, **67**, 374 (1995).
4. L. F. Gosset, J.-J. Ganem, I. Trimaille, S. Rigo, F. Rochet, G. Dufour, F. Jolly, F. C. Stedile, and I. J. R. Baumvol, *Nucl. Instrum. Methods Phys. Res. B*, **136-138**, 521 (1998).
5. M. R. Frost and C. W. Magee, *Appl. Surf. Sci.*, **104/105**, 379 (1995).
6. S. Iwata and A. Ishizaka, *J. Appl. Phys.*, **79**, 6653 (1996).
7. Z.-H. Lu, J. P. McCaffrey, B. Brar, G. D. Wilk, R. M. Wallace, L. C. Feldman, and S. P. Tay, *Appl. Phys. Lett.*, **71**, 2764 (1997).
8. B. Hajji, P. Temple-Boyer, F. Olivié, and A. Martinez, *Thin Solid Films*, **354**, (1999).
9. D. Landheer, K. Rajesh, D. P. Masson, J. E. Hulse, G. I. Sproule, and T. Quance, *J. Vac. Sci. Technol. A*, **16**, 2931 (1998).
10. J. C. Chang, T. Nguyen, J. S. Nakos, and J. F. Korejwa, in *Rapid Thermal and Integrated Processing*, SPIE **1595**, 35 (1991); SPIE-Int. Soc. Opt. Instrumentation Eng.
11. S. Tougaard, *Surf. Interface Anal.*, **25**, 137 (1997), and references cited therein.
12. L. C. Feldman and J. W. Mayer, *Fundamentals of Surface and Thin Film Analysis*, North-Holland, Amsterdam (1982).
13. M. F. Hochella, Jr. and A. H. Carim, *Surf. Sci.*, **197**, L260 (1988).
14. M. P. Seah and W. A. Dench, *Surf. Interface Anal.*, **1**, 2 (1979).
15. S. Tanuma, C. J. Powell, and D. R. Penn, *Surf. Interface Anal.*, **17**, 927 (1991).
16. R. Flitsch and S. I. Raider, *J. Vac. Sci. Technol.*, **12**, 305 (1975).
17. D. Landheer, P. Ma, W. N. Lennard, I. V. Mitchell, and C. McNorgan, *J. Vac. Sci. Technol. A*, **18**, 2503 (2000).
18. V. A. Gritsenko, J. B. Xu, R. W. M. Kwok, Y. H. Ng, and I. H. Wilson, *Phys. Rev. Lett.*, **81**, 1054 (1998).
19. J. R. Hauser and K. Ahmed, in *Characterization and Metrology for ULSI Technology: 1998 International Conference Proceedings*, D. G. Seiler, A. C. Diebold, W. M. Bullis, T. J. Shaffner, R. McDonald, and E. J. Walters, Editors, pp. 235-239, The American Institute of Physics, New York (1998).

20. R. J. Hussey, T. L. Hoffman, Y. Tao, and M. J. Graham, *J. Electrochem. Soc.*, **143**, 221 (1996).
21. R. A. Hegde, B. Maiti, and P. J. Tobin, *J. Electrochem. Soc.*, **144**, 1081 (1997), and references cited therein.
22. D. Bouvet, P. A. Clivaz, M. Dutoit, C. Coluzza, J. Almeida, G. Margaritondo, and F. Pio, *J. Appl. Phys.*, **79**, 7114 (1996).
23. D. G. J. Sutherland, H. Akatsu, M. Kopel, F. J. Himpsel, T. A. Callcott, J. A. Carlisle, D. L. Ederer, J. J. Jia, I. Jimenez, R. Perera, D. K. Shuh, L. J. Terminello, and W. M. Tong, *J. Appl. Phys.*, **78**, 6761 (1995).
24. S. I. Raider, R. Flitsch, J. A. Aboaf, and W. A. Pliskin, *J. Electrochem. Soc.*, **123**, 560 (1976).
25. W. Ting, H. Hwang, J. Lee, and D. L. Kwong, *Appl. Phys. Lett.*, **57**, 2808 (1990).
26. B. Brar, G. D. Wilk, and A. C. Seabaugh, *Appl. Phys. Lett.*, **69**, 2728 (1996).